

Dopant profile engineering by near-infrared femtosecond laser activation

Yi-Chao Wang, Ci-Ling Pan, Jia-Min Shieh, and Bau-Tong Dai

Citation: [Applied Physics Letters](#) **88**, 131104 (2006); doi: 10.1063/1.2191095

View online: <http://dx.doi.org/10.1063/1.2191095>

View Table of Contents: <http://scitation.aip.org/content/aip/journal/apl/88/13?ver=pdfcov>

Published by the [AIP Publishing](#)

Articles you may be interested in

[Active dopant profiling of ultra shallow junction annealed with combination of spike lamp and laser annealing processes using scanning spreading resistance microscopy](#)

[AIP Conf. Proc.](#) **1496**, 164 (2012); 10.1063/1.4766515

[Enhancement of phosphorus activation in vacancy engineered thin silicon-on-insulator substrates](#)

[J. Appl. Phys.](#) **106**, 103514 (2009); 10.1063/1.3262527

[Dopant activation in subamorphized silicon upon laser annealing](#)

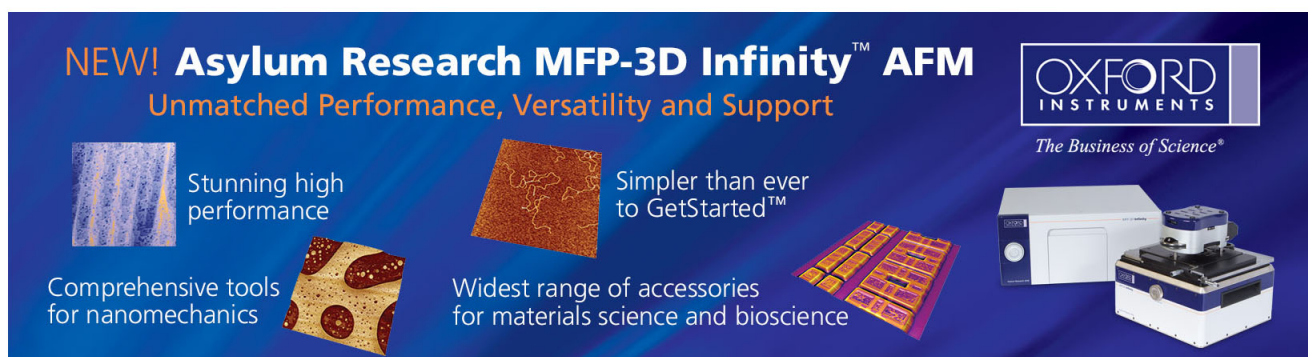
[Appl. Phys. Lett.](#) **89**, 082101 (2006); 10.1063/1.2335950

[Electrical activation phenomena induced by excimer laser annealing in B-implanted silicon](#)

[Appl. Phys. Lett.](#) **85**, 2268 (2004); 10.1063/1.1793352

[Redistribution and electrical activation of ultralow energy implanted boron in silicon following laser annealing](#)

[J. Vac. Sci. Technol. B](#) **20**, 644 (2002); 10.1116/1.1459725

The advertisement features a dark blue background with white and orange text. At the top left, it reads 'NEW! Asylum Research MFP-3D Infinity™ AFM' in large white letters, followed by 'Unmatched Performance, Versatility and Support' in orange. To the right is the Oxford Instruments logo, which includes the text 'OXFORD INSTRUMENTS' and the tagline 'The Business of Science®'. Below the main text are four images: a textured surface, a circular pattern, a grid of small squares, and the AFM instrument itself. Each image is accompanied by a short text description: 'Stunning high performance', 'Simpler than ever to GetStarted™', 'Comprehensive tools for nanomechanics', and 'Widest range of accessories for materials science and bioscience'.

Dopant profile engineering by near-infrared femtosecond laser activation

Yi-Chao Wang and Ci-Ling Pan^{a)}

Department of Photonics and Institute of Electro-Optical Engineering, National Chiao Tung University, Hsinchu 30010, Taiwan, Republic of China

Jia-Min Shieh and Bau-Tong Dai

National Nano Device Laboratories, Hsinchu 30078, Taiwan, Republic of China

(Received 23 August 2005; accepted 7 March 2006; published online 28 March 2006)

Femtosecond laser annealing (FLA) was employed for activation of phosphorus (P)- and boron (B)-implanted silicons with negligible dopant diffusion. Preamorphizing implantation is not required. We found that the dopant profiles in FLA-activated samples essentially duplicate those of as-implanted ones even for junctions as deep as 100 nm below the surface. The measured sheet resistances and activation efficiencies of P- and B-implanted samples were in the range of 100–400 Ω/\square and 28%–35%, respectively. Moreover, thermal-energy-assisted dopant diffusion by heating was observed for substrate temperature as low as 100 °C. The shallow activated-depth feature associated with FLA reduces the separation between end-of-range defects and high-concentration portion of dopants. This generates a steep interstitial gradient responsible for observed B and P uphill diffusions at a depth of about 60 nm below the surface. © 2006 American Institute of Physics. [DOI: 10.1063/1.2191095]

Much effort has been focused on the formation of thin insulators, short channels, and shallow junctions by dopant profiling^{1–6} for scaling of transistor-based silicon devices to ~100 nm. State-of-the-art dopant profile engineering is achieved by integrating low-energy implantation,^{1,2} defect engineering,^{3–6} and fast solid phase epitaxial regrowth^{2,4} or laser annealing.^{4–6} To date, dopant profile engineering still faces challenges such as boron-enhanced diffusion (BED),¹ transient-enhanced diffusion (TED),² boron-interstitial clustering,² and uphill diffusion.^{3,6,7} In comparison, activation by nanosecond excimer laser annealing^{4–6,8,9} (ELA) can more effectively minimize dopant diffusion than furnace annealing⁴ (FA) and spiked rapid thermal processing (RTP).^{4,7,8,10} Nevertheless, dopant diffusion during ELA-based activation is not eliminated altogether. This is generally attributed to both vacancy-mediated^{3,6,7} and interstitial-mediated^{1,2} diffusion mechanisms that are enhanced by a rapid melting and solidification process. Recently, we reported femtosecond laser ($\lambda=800$ nm) annealing (FLA) of amorphous silicon (*a*-Si).¹¹ In this work, we report FLA-activated *n*-type (phosphorous or P) and *p*-type (boron or B) dopants confined in ultrashallow junction regions. Preamorphization by implantation (PAI) is not required.

We employed a 1 kHz Ti:sapphire regenerative amplifier ($\lambda=800$ nm), generating 50 fs pulses, and a line-scan FLA (Ref. 11) to activate P- or B-implanted Si substrates. To compare, PAI by Si⁺ as well as the use of BF₂⁺ instead of B⁺ for implantation were employed for some of the samples. ELA-activation experiments using a KrF laser ($\lambda=238$ nm) were also conducted. The samples and processing parameters studied are summarized in Table I. Dopant profiles for activated and as-implanted samples were analyzed by secondary ion mass spectrometry (SIMS) and spreading resistance profiling (SRP) for assessment of the active and retained dose. Sheet resistances of all samples were measured by using a four-point probe.

Figure 1 shows SIMS profiles of borons in B-implanted layers without (sample A) and with PAI (sample B) as well as BF₂⁺-implanted layers (sample C). Junction depths for the three as-implanted samples were designed to be 270, 200, and 100 nm, respectively. The SIMS and SRP measurements of boron in low-energy B-implanted layers (sample C) and phosphorus in low-energy P-implanted layers with a junction depth of 100 nm (sample D) are shown in Figs. 2 and 3. Laser fluences required for activating all the samples were 27–39, vs 45 mJ/cm² for FLA crystallization of *a*-Si films.¹¹ Sheet resistances for all FLA-activated samples were in the range of 100–400 Ω/\square .

After FLA activation at room temperature (24 °C), dopant profiles of all activated samples were found to be almost the same as those of as-implanted ones (see Figs. 1 and 2). No flat-top profiles were observed in regions of highly concentrated dopants, as opposed to the cases for activation by ELA.^{4–6,8,9} This likely implies the absence of dopant redistribution by FLA activation. The laser fluence required for FLA activation is 0.5 J/cm², much lower than that for ELA activation (5–10 J/cm²).^{5,8} Either linear or nonlinear absorption of laser photons by implanted samples is not expected to reduce the required activation fluence. The low fluence required for FLA activation thus suggests that ultrafast or nonthermal melting of semiconductors^{12,13} is the dominant mechanism. Irradiated by femtosecond pulses that photoexcited a large enough fraction of the valence electrons in the semiconductor, the lattice is weakened and a structural change can occur while the electronic systems of the lattice are not in thermal equilibrium with each other. Such a nonthermal melting mechanism could minimize dopant diffusion significantly by reducing the thermal budget of activation.⁴

For FLA activation of samples at room temperature, we show in Fig. 1 that dopant diffusion after activation is negligible in samples A and B. The peak position in B dopant profile of sample C after FLA activation, however, shifts by about 10 nm with respect to that of as-implanted sample C.

^{a)}Electronic mail: clpan@faculty.nctu.edu.tw

TABLE I. Implantation parameters and FLA-activation and ELA-activation conditions for three B-doped and P-doped layers. Sheet resistances for doped layers activated by FLA with those activated by ELA methods in this work and reported in Refs. 4 and 5 are listed for comparison. Dopant depth is defined as the distance from the surface at which the dopant concentrations drop to 10^{18} cm^{-3} .

	B-implanted <i>a</i> -Si (without PAI)	B-implanted Si (with PAI)	BF ₂ ⁺ -implanted Si	P-implanted Si
Si PAI parameters		50 keV $5 \times 10^{15} \text{ cm}^{-2}$		
Dopant implantation parameters	20 keV $5 \times 10^{15} \text{ cm}^{-2}$	20 keV $5 \times 10^{15} \text{ cm}^{-2}$	25 keV $5 \times 10^{15} \text{ cm}^{-2}$	15 keV $5 \times 10^{15} \text{ cm}^{-2}$
Fluence used for FLA (ELA) (mJ/cm ²)	37–39	30–34	27–29 (250)	31–33 (250)
Number of laser shots for FLA (ELA)	20	20	20 (20)	20 (20)
Junction depth (as implanted) (nm)	~270	~200	~100	~100
Sheet resistance of FLA-activated samples (Ω/\square)	100–250	200–400	225–450	225–325
Sheet resistance of RTA-activated samples (Ω/\square)		280–300 ^a		
Sheet resistance of ELA-activated samples (Ω/\square)		190–300 ^{a,b}	180 ^c	160 ^c

^aReference 4.

^bReference 5.

^cThis work.

This is independent of the substrate temperature up to 200 °C. We also observed uphill diffusion towards the surface by ~10 nm for sample C at profile depth beyond ~60 nm. Uphill diffusion is more apparent at elevated substrate temperatures. In samples A and B, on the other hand, no uphill diffusion was observed. We note that uphill diffusion in dopant profiles for silicon activated by other methods often occurs at a depth as shallow as 10 nm.^{3,6,14} For P dopant profiles in sample D without substrates heating (see Fig. 3), uphill diffusion at a depth of 60 nm is barely observable,

whereas P atoms diffuse away from the surface by ~10 nm at elevated temperatures.

Electrical profiling (SRP) of active B and P in samples C and D, respectively, were conducted and shown in Figs. 2 and 3. Increasing the substrate temperature from 24 °C to 200 °C, the activation efficiency (dose activated/dose implanted) of sample C (D) increases from 28% (31%) to 33% (36%). At the same time, the sheet resistance of sample C (D) decreases from 450(325) to 225(225) Ω/\square . These values are similar to reported ELA results.⁸ Uphill

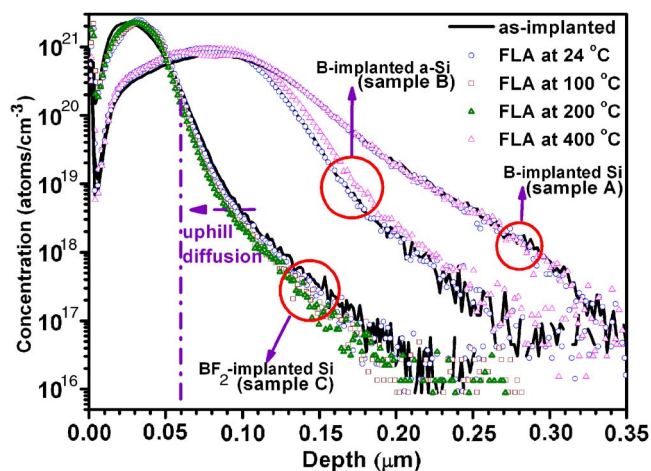


FIG. 1. (Color online) SIMS profiles of as-implanted B-doped samples with (sample A) and without PAI (sample B) as well as BF₂⁺-implanted samples (sample C). SIMS profiles for all B-doped layers activated by FLA at different substrate temperatures are also shown.

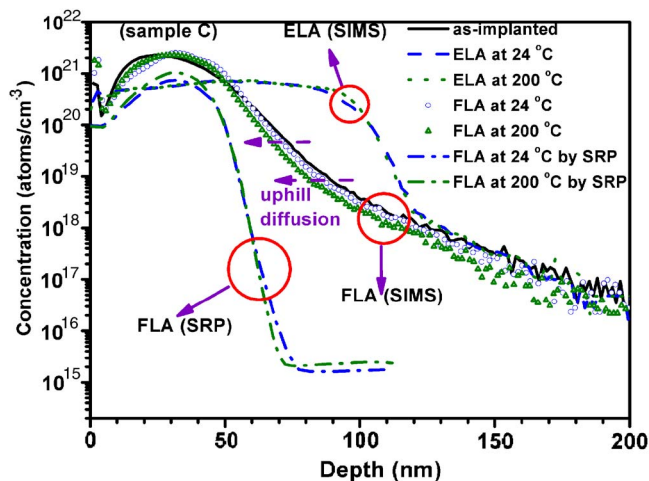


FIG. 2. (Color online) SIMS profiles for BF₂⁺-implanted layers activated by either FLA or ELA at different substrate temperatures. SRP profiles for BF₂⁺-implanted layers activated by FLA at different temperature are also shown.

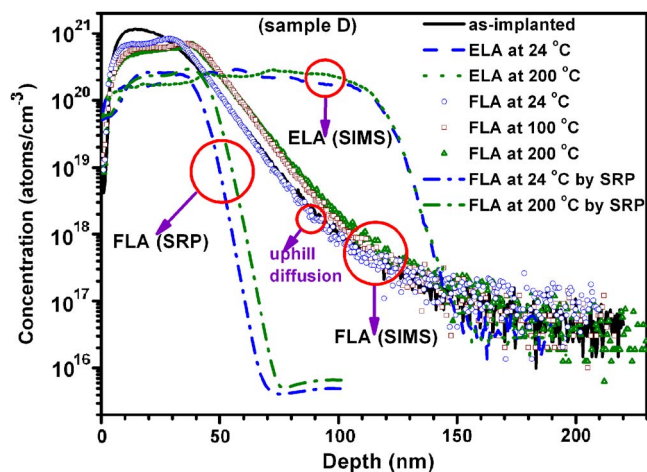


FIG. 3. (Color online) SIMS and SRP profiles for P-implanted layers activated by FLA at different substrate temperatures. SIMS profiles for P-implanted layers activated by ELA at different substrate temperatures are also shown. The dopant depth was designed to be the same as for BF_2^+ -implanted samples.

diffusion of boron atoms is also apparent in SRP curves for sample C FLA activated at 24 and 200 °C (see Fig. 2). In the same figure, we show the flat-top profiles of ELA activation for sample C at 24 and 200 °C. Uphill diffusion phenomena in ELA-activated samples C and D are not observed. This is also shown in Figs. 2 and 3. It is obvious that, in the melting regime, ELA obliterates any effect of substrate temperature. One might consider comparing nonmelting ELA performed at 200 °C with FLA at the same temperature. For the former case, it is reported that boron exhibited negligible diffusion during each pulse and the sheet resistance values could not be measured by the four-point probe because the values were too high.⁵ That is, activation by nonmelting ELA is ineffective, while we have shown that FLA activation is very successful.

Using femtosecond laser pulses, ultrafast or nonthermal melting of the sample surface rather than heat penetration due to thermal conduction¹³ is expected to lead to a thinner melting depth in FLA-annealed samples. This limits the activation depth and thus prevents thermally assisted diffusion of end-of-range (EOR) defects further away from the surfaces. As a result, trapped interstitials will remain within the EOR regions for FLA, accomplishing the functionality of PAI in ELA.^{3,6} This model is corroborated by the observation of a steep slope around the depth of 50–70 nm for the observed SRP profiles. Recently, Duffy and co-workers^{3,14} reported that uphill diffusion during low-temperature (700 °C) furnace annealing was driven by an interstitial gradient between the EOR region and high-concentration portion of the dopant profile.¹⁴ This gradient is steeper when the distance between the two regions is reduced by PAI control or if the amorphous-crystalline (*a/c*) interface is shallow. As a result, a high concentration of boron-interstitial pairs is likely to form during annealing.³ Boron atoms move appreciably toward the surface consequently. The *a/c* interface for samples C and D with implanted depth of 100 nm is much closer to the surface than that for samples A and B with implanted depth of 200–270 nm. The former two samples are thus expected to be influenced more by the FLA-induced PAI-like effects than the latter two.

Heating of the samples during activation will render the interstitials more mobile.⁶ For BF_2^+ -doped layers, elevated substrate temperature likely facilitates the generation of more boron-interstitial pairs, thereby promoting B uphill diffusion.³ Uphill diffusion of P atoms in shallow P-implanted layers FLA activated at elevated substrate temperature were not observed (see Figs. 2 and 3). The diffusivity of P atoms doped is much higher than that of B atoms in Si,¹⁵ underlying the different behavior for B and P and consistent with observation that the dopant profile of the P-implanted layer is broader than that of the BF_2^+ -implanted sample for ELA activation.

In summary, femtosecond laser annealing (FLA) was employed for activation of P- and B-implanted silicons with negligible dopant diffusion. Preamorphization by implantation, commonly used in conventional activation schemes for minimizing the diffusion of dopant during annealing, is not required. We find dopant profiles in FLA-activated samples essentially duplicate those of as-implanted ones even for junctions as deep as 100 nm below the surface. The measured sheet resistances and activation efficiencies of P- and B-implanted samples were in the range of 100–400 Ω/\square and 28%–35%, respectively. Moreover, thermal-energy-assisted dopant diffusion by heating was observed for substrate temperature as low as 100 °C. The shallow activated-depth feature associated with FLA reduces the separation between end-of-range defects and high-concentration portion of dopants. This generates a steep interstitial gradient responsible for observed B and P uphill diffusions at a depth of about 60 nm below the surface.

This work was supported in part by various grants funded by the National Science Council, Taiwan, Republic of China. The authors also thank Zun-Hao Chen for technical assistance.

¹A. Agarwal, H. J. Gossmann, D. J. Eaglesham, S. B. Hermer, A. T. Fiory, and T. E. Haynes, *Appl. Phys. Lett.* **74**, 2435 (1999).

²A. Agarwal, H. J. Gossmann, D. J. Eaglesham, L. Pelaz, D. C. Jacobson, T. E. Haynes, and Y. Erokhin, *Appl. Phys. Lett.* **71**, 3141 (1997).

³R. Duffy, V. C. Venezia, A. Heringa, T. W. T. Husken, M. J. P. Hopstaken, N. E. B. Cowern, P. B. Griffin, and C. C. Wang, *Appl. Phys. Lett.* **82**, 3647 (2003).

⁴Y. F. Chong, K. L. Pey, A. T. S. Wee, A. See, L. Chan, Y. F. Lu, W. D. Song, and L. H. Chua, *Appl. Phys. Lett.* **76**, 3197 (2000).

⁵C. H. Poon, B. J. Cho, Y. F. Lu, M. Bhat, and Alex See, *J. Vac. Sci. Technol. B* **21**, 706 (2003).

⁶C. H. Poon, L. S. Tan, B. J. Cho, A. See, and M. Bhat, *J. Electrochem. Soc.* **151**, G80 (2004).

⁷H. C. H. Wang, C. C. Wang, C. S. Chang, T. Wang, P. B. Griffin, and C. H. Diaz, *IEEE Electron Device Lett.* **22**, 65 (2001).

⁸V. Privitera, C. Spinella, G. Fortunato, and L. Mariucci, *Appl. Phys. Lett.* **77**, 552 (2000).

⁹S. Whelan, A. L. Magna, V. Privitera, G. Mannino, M. Italia, C. Bongiorno, G. Fortunato, and L. Mariucci, *Phys. Rev. B* **67**, 075201 (2003).

¹⁰L. Shao, X. Wang, I. Rusakova, H. Chen, J. Liu, J. Bennett, L. Larson, J. Jin, P. A. W. van der Heide, and W. K. Chu, *J. Appl. Phys.* **92**, 5788 (2002).

¹¹J. M. Shieh, Z. H. Chen, B. T. Dai, Y. C. Wang, A. Zaitsev, and C. L. Pan, *Appl. Phys. Lett.* **85**, 1232 (2004).

¹²S. K. Sundaram and E. Mazur, *Nat. Mater.* **1**, 217 (2002).

¹³A. Rousse, C. Rischel, S. Fourmaux, I. Uschmann, S. Sebban, G. Grillon, Ph. Balcou, E. Förster, J. P. Geindre, P. Audebert, J. C. Gauthier, and D. Hulin, *Nature (London)* **410**, 65 (2001).

¹⁴R. Duffy, V. C. Venezia, J. Loo, M. J. P. Hopstaken, M. A. Verheijen, G. C. J. Maas, Y. Tamminga, T. Dao, and C. Demeurisse, *Appl. Phys. Lett.* **86**, 81917 (2005).

¹⁵J. Xu, V. Krishnamoorthy, K. S. Jones, and M. E. Law, *J. Appl. Phys.* **81**, 107 (1997).